

Cervical cord myelin abnormality is associated with clinical disability in multiple sclerosis

Lisa Eunyoung Lee* , Irene M Vavasour*, Adam Dvorak , Hanwen Liu, Shawna Abel , Poljanka Johnson, Stephen Ristow, Shelly Au, Cornelia Laule, Roger Tam, David KB Li, Helen Cross, Nathalie Ackermans, Alice J Schabas, Jillian Chan, Ana-Luiza Sayao, Virginia Devonshire, Robert Carruthers , Anthony Traboulsee and Shannon Kolind

Abstract

Background: Myelin water imaging (MWI) was recently optimized to provide quantitative in vivo measurement of spinal cord myelin, which is critically involved in multiple sclerosis (MS) disability.

Objective: To assess cervical cord myelin measurements in relapsing-remitting multiple sclerosis (RRMS) and progressive multiple sclerosis (ProgMS) participants and evaluate the correlation between myelin measures and clinical disability.

Methods: We used MWI data from 35 RRMS, 30 ProgMS, and 28 healthy control (HC) participants collected at cord level C2/C3 on a 3 T magnetic resonance imaging (MRI) scanner. Myelin heterogeneity index (MHI), a measurement of myelin variability, was calculated for whole cervical cord, global white matter, dorsal column, lateral and ventral funiculi. Correlations were assessed between MHI and Expanded Disability Status Scale (EDSS), 9-Hole Peg Test (9HPT), timed 25-foot walk, and disease duration.

Results: In various regions of the cervical cord, ProgMS MHI was higher compared to HC (between 9.5% and 31%, $p \leq 0.04$) and RRMS (between 13% and 26%, $p \leq 0.02$), and ProgMS MHI was associated with EDSS ($r = 0.42-0.52$) and 9HPT ($r = 0.45-0.52$).

Conclusion: Myelin abnormalities within clinically eloquent areas are related to clinical disability. MWI metrics have a potential role for monitoring subclinical disease progression and adjudicating treatment efficacy for new therapies targeting ProgMS.

Keywords: Multiple sclerosis, spinal cord, magnetic resonance imaging, quantitative MRI, myelin water imaging, demyelination

Date received: 8 February 2021; revised: 8 February 2021; accepted: 21 February 2021

Introduction

A non-invasive, quantitative measurement of spinal cord pathology would be clinically valuable, given its critical involvement in motor, sensory, and autonomic deficits in multiple sclerosis (MS). One promising quantitative magnetic resonance imaging (MRI) approach is myelin water imaging (MWI), which can be performed using multi-component T2 relaxation analysis to quantify the magnetic resonance (MR) signal from different water environments within each voxel.¹ Healthy central nervous system tissue typically demonstrates two components, intra- and

extracellular water (T2 ~70 ms) and myelin water located between myelin bilayers (T2 ~15 ms).¹ The myelin water fraction (MWF) is defined as the fraction of MR signal from myelin water to the total water.¹ MWF has been histopathologically validated as an in vivo marker of myelin and applied to study myelin abnormalities in various neurological diseases including MS.²⁻⁴

While the majority of publications have focused on the brain, recent studies have shown robust myelin measurements in the spinal cord of healthy volunteers

Multiple Sclerosis Journal
2021, Vol. 27(14) 2191–2198

DOI: 10.1177/
13524585211001780

© The Author(s), 2021.



Article reuse guidelines:
sagepub.com/journals-
permissions

Correspondence to:

SH Kolind

Division of Neurology,
Department of Medicine,
The University of British
Columbia, S199-2211
Westbrook Mall, Vancouver,
BC V6T 2B5, Canada.
shannon.kolind@ubc.ca

Lisa Eunyoung Lee

Shawna Abel

Poljanka Johnson

Stephen Ristow

Shelly Au

Helen Cross

Nathalie Ackermans

Alice J Schabas

Jillian Chan

Ana-Luiza Sayao

Virginia Devonshire

Robert Carruthers

Anthony Traboulsee

Division of Neurology,
Department of Medicine,
The University of British
Columbia, Vancouver, BC,
Canada

Irene M Vavasour

Roger Tam

Department of Radiology,
The University of British
Columbia, Vancouver, BC,
Canada

David KB Li

Division of Neurology,
Department of Medicine,
The University of British
Columbia, Vancouver,
BC, Canada/Department of
Radiology, The University
of British Columbia,
Vancouver, BC, Canada

Adam Dvorak

Hanwen Liu

Department of Physics and
Astronomy, The University
of British Columbia,
Vancouver, BC, Canada;
International Collaboration
on Repair and Discoveries,
Vancouver, BC, Canada

Cornelia Laule

Department of Radiology, The University of British Columbia, Vancouver, BC, Canada; Department of Physics and Astronomy, The University of British Columbia, Vancouver, BC, Canada; International Collaboration on Repair and Discoveries, Vancouver, BC, Canada; Department of Pathology and Laboratory Medicine, The University of British Columbia, Vancouver, BC, Canada

Shannon Kolind

Division of Neurology, Department of Medicine, The University of British Columbia, Vancouver, BC, Canada; Department of Radiology, The University of British Columbia, Vancouver, BC, Canada; Department of Physics and Astronomy, The University of British Columbia, Vancouver, BC, Canada; International Collaboration on Repair and Discoveries, Vancouver, BC, Canada

*The authors contributed equally to the manuscript.

and disease pathology using MWI.^{5,6} In this study, we investigated the myelin heterogeneity index (MHI), calculated as the MWF standard deviation divided by the mean within a region of interest (ROI). MHI increases during demyelination, as both the variability of MWF increases and the mean MWF decreases, providing superior sensitivity in distinguishing myelin abnormality from normal inter-individual variability. We investigated whether (1) cervical cord myelin was more variable in MS compared to healthy controls (HCs) and (2) the degree of cervical cord myelin heterogeneity reflected clinical symptoms within ROIs.

Methods

Study participants

Forty-one relapsing-remitting multiple sclerosis (RRMS), 38 progressive multiple sclerosis (ProgMS), and 31 age- and sex-matched HC participants with no previously known neurological disorders participated in the study. All MS participants fulfilled the 2017 revised McDonald diagnostic criteria.⁷ Participants were excluded if they had active infectious disease or a history of neurological conditions other than MS. RRMS participants treated with fingolimod or monoclonal antibodies at the time of baseline scan were excluded from the study. MS participants, who were treated with glatiramer acetate, dimethyl fumarate, teriflunomide, interferon beta, or steroids at the time of visit, were included in the study. Participants were recruited either online, via advertisement on local health authority websites, or in person through the University of British Columbia Hospital MS Clinic. All participants provided written informed consent prior to participation. This study was approved by the clinical research ethics board at the University of British Columbia (H17-00866).

Clinical assessments

Kurtzke's Expanded Disability Status Scale (EDSS) score⁸ was evaluated by a trained neurologist, who completed Neurostatus training. Timed 25-foot walk (T25W) assessed ambulation by measuring the amount of time required for walking a distance of 25 feet as quickly as possible.⁹ Nine-Hole Peg Test (9HPT) assessed upper limb function by measuring the amount of time required to individually insert pegs into each of the nine holes then removing them.⁹ Disease duration was defined as the period of the disease course since the onset of first symptoms.

MRI data acquisition

MRI data were acquired on a Philips Achieva 3.0T scanner (Philips Medical Systems, Best, The Netherlands) using a 6-channel spine coil at the University of British Columbia MRI Research Center. T2 relaxation MWI data were obtained using a 3D gradient and spin echo (GRASE) sequence (32 echoes, TE = 10 ms, TR = 1500 ms, eight slices acquired at $0.75 \times 0.75 \times 5 \text{ mm}^3$ reconstructed to 16 slices at $0.63 \times 0.63 \times 2.5 \text{ mm}^3$, field of view (FOV) = $180 \times 150 \times 40 \text{ mm}^3$, SENSE factor = 2, acquisition time = 8.5 min) in the cervical spinal cord.¹⁰ A high-resolution T2*-weighted multi-echo fast gradient echo (mFFE) sequence (5 echoes, TE1 = 6.5 ms, $\Delta\text{TE} = 8.2 \text{ ms}$, TR = 809 ms, 16 slices, acquired at $0.8 \times 0.8 \times 2.5 \text{ mm}^3$ reconstructed to $0.3 \times 0.3 \times 2.5 \text{ mm}^3$, FOV = $150 \times 150 \times 44 \text{ mm}^3$, acquisition time = 5 min) was acquired for tissue segmentation and image registration. Axial scans were centered at the level of the C2/C3 intervertebral disk with the image plane perpendicular to the longitudinal axis of the cord.

Data analysis

The 32-echo GRASE T2 decay curves were analyzed using regularized non-negative least squares with the extended phase graph algorithm and stimulated echo correction to obtain voxel-wise T2 distributions (40 logarithmically spaced T2 values from 15 to 2000 ms).^{1,10,11} Signal with a T2 relaxation time under 40 ms was attributed to myelin water. Voxel-wise MWF maps were computed as the ratio of the myelin water signal to the total water signal.¹ T2 analysis was performed using in-house software code (analysis program available from this URL: <https://mriresearch.med.ubc.ca/news-projects/myelin-water-fraction/>) developed at the University of British Columbia.¹²

Image registration and tissue segmentation were performed using the Spinal Cord Toolbox (SCT) 3.2.7.¹³ The spinal cord and gray matter were segmented using `sct_deepseg_sc` and `sct_deepseg_gm` tools, respectively. SCT 3.1.0 was used for `sct_register_graymatter`. Whole cervical cord and global white matter (WM) masks were extracted from the mFFE image. Three isolated ROIs of the dorsal column, lateral funiculi, and ventral funiculi were obtained using an iterative, non-linear registration to transform the PAM50 spinal cord template from standard space to mFFE space (Figure 1).¹⁴ This provided probabilistic ROIs, which were thresholded to only include voxels with probability greater than 0.5 to reduce partial volume effects. ROIs were then visually inspected to

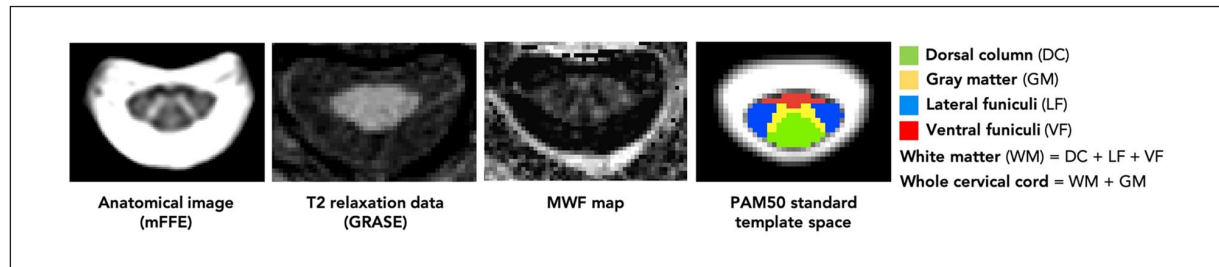


Figure 1. An example of cervical cord images at the C2/C3 level of a progressive multiple sclerosis participant. Images include multi-echo fast gradient echo (mFFE), gradient and spin echo (GRASE), myelin water fraction (MWF) map, and regions of interest on PAM50 standard template space.

Table 1. Clinical and demographic information of the participants.

Group	Sex (% female)	Mean age (range) (years)	Mean disease duration (range) (years)	Median EDSS (range)	Mean 9HPT (range) (seconds)	Mean T25W (range) (seconds)
HC ($n=28$)	10M/18F (64)	45 (27–65)	N/A	N/A	N/A	N/A
RRMS ($n=35$)	9M/26F (74)	44 (26–61)	11 (0.3–48)	2.5 (1.0–6.0)	20.1 (14.2–31.6)	4.4 (3.2–6.4)
ProgMS ($n=30$)	11M/19F (63)	57 (48–65)	22 (1–43)	4.0 (2.0–7.5)	25.4 (17.1–47.7)	6.7 (3.1–13.3)
PPMS ($n=11$)						
SPMS ($n=19$)						

RRMS: relapsing-remitting multiple sclerosis; ProgMS: progressive multiple sclerosis; HC: healthy control; PPMS: primary-progressive multiple sclerosis; SPMS: secondary-progressive multiple sclerosis; EDSS: Expanded Disability Status Scale; N/A: not applicable.

From the original study cohort of 41 RRMS, 38 ProgMS, and 31 HC, 6 RRMS, 8 ProgMS, and 3 HC were excluded in the analysis due to imaging artifacts.

ensure high-quality registration, absence of pulsation artifacts from cerebrospinal fluid (CSF) flow and correct anatomical coverage. For our purposes of assessing global myelin abnormalities in each ROI, ROIs included both lesion and normal-appearing white matter (NAWM) tissue. MHI (myelin heterogeneity) was calculated within each ROI for the 10 middle slices due to potential wrap-around artifact in the furthest rostral or caudal slices of the imaging volume.

Statistical analysis

A one-way analysis of variance (ANOVA) with Tukey post hoc test for multiple comparisons was performed to compare MHI in the cervical cord between RRMS, ProgMS, and HC. Spearman's rank correlation coefficient was used to assess relationships between MHI and clinical disability. $P \leq 0.05$ was reported as significant. Statistical analyses were conducted in *R* version 3.3.3.

Results

Table 1 displays the participant demographic and clinical information including sex, age, disease duration, EDSS, 9HPT, and T25W. Data from six RRMS, eight ProgMS, and three HC were excluded due to imaging artifacts, resulting in the including of

imaging data from 35 RRMS, 30 ProgMS, and 28 HC. EDSS data were unavailable for two participants due to time restrictions. 9HPT and T25W data were unavailable for 8 and 13 participants, respectively, as they could not perform these tasks due to their disability (e.g. wheelchair dependent) or time restrictions.

Compared to HC, ProgMS MHI was higher in the whole cervical cord (+9.5%, $p=0.04$), global WM (+19%, $p=0.0009$), dorsal column (+31%, $p<0.0001$) and lateral funiculi (+17%, $p=0.01$; Figure 2). ProgMS did not differ from HC in MHI of the ventral funiculi. ProgMS had a higher MHI compared to RRMS in global WM (+13%, $p=0.02$) and dorsal column (+26%, $p<0.0001$), with trends in whole cervical cord and lateral funiculi (Figure 2). RRMS was not significantly different from HC in any region.

As seen in Figure 3, when all MS participants were included, MHI correlated with EDSS in global WM ($r=0.35$, $p=0.005$), dorsal column ($r=0.36$, $p=0.004$), and lateral funiculi ($r=0.33$, $p=0.009$). MHI also correlated with 9HPT in whole cervical cord ($r=0.40$, $p=0.002$), global WM ($r=0.47$, $p=0.0002$), dorsal column ($r=0.52$, $p<0.0001$), and lateral funiculi ($r=0.32$, $p=0.02$). Finally, MHI correlated with disease duration in global WM ($r=0.31$, $p=0.01$), dorsal column ($r=0.24$, $p=0.05$), and

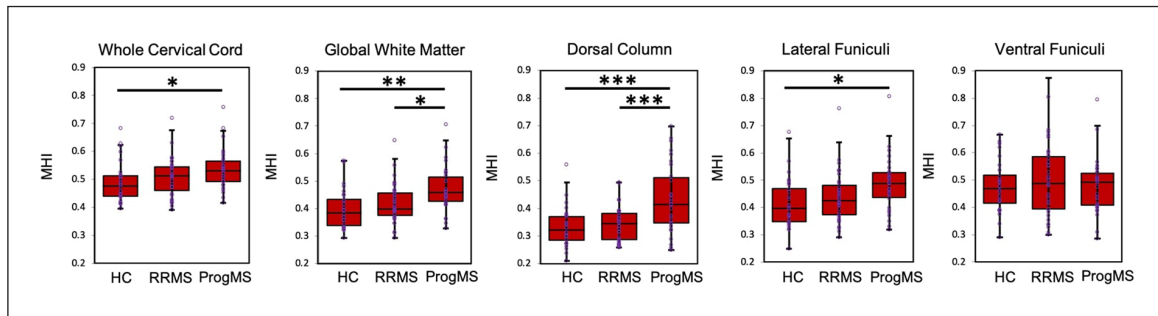


Figure 2. Myelin heterogeneity index (MHI) was compared between healthy controls (HCs), relapsing-remitting multiple sclerosis (RRMS), and progressive multiple sclerosis (ProgMS). Regions of interest included whole cervical cord, global white matter, dorsal column, lateral funiculi and ventral funiculi.

Significant differences are indicated with $*p < 0.05$, $**p < 0.005$, $***p < 0.0005$. Please note that to keep a uniform y-axis scale, one data point (MHI = 1.19 in an RRMS participant) from the Ventral Funiculi plot is not shown.

lateral funiculi ($r = 0.30$, $p = 0.02$). RRMS alone showed no significant correlations. ProgMS had stronger correlations when RRMS were removed between MHI and EDSS in whole cervical cord ($r = 0.52$, $p = 0.004$), global WM ($r = 0.42$, $p = 0.02$), and lateral funiculi ($r = 0.46$, $p = 0.01$) and between MHI and 9HPT in whole cervical cord ($r = 0.48$, $p = 0.01$), global WM ($r = 0.45$, $p = 0.02$) and dorsal column ($r = 0.52$, $p = 0.005$). No significant correlations were found between MHI and T25W.

Discussion

In this study, we used a novel myelin-related MRI metric to characterize the degree of myelin abnormality in the cervical cord of RRMS and ProgMS, and probe if that myelin abnormality was related to clinical measures. We found a higher MHI in ProgMS compared to RRMS and HC. There were significant correlations between MHI and clinical disability, as measured by EDSS and 9HPT, that were best appreciated in ProgMS. The correlations were not being driven by a bi-modal distribution with separate clumps of patient groups. In order to determine a sufficient sample size to have detected a significant difference in MHI between RRMS and HC for each ROI, we performed power analyses using the MHI mean and standard deviation from Table 2. Using the G*Power program (version 3.1.9.3), a sample of 112 (lateral funiculi), 153 (whole cervical cord and global WM), 255 (ventral funiculi) and 527 (dorsal column) in each group would be needed to achieve 80% power using a two-sample independent t -test with alpha at 0.05.

A previous study by Kolind et al.¹⁵ using another myelin-sensitive technique (mcDESPOT) reported a similar association between mean MWF in cervical cord

and EDSS ($r = -0.53$, $p = 0.04$) and 9HPT ($r = 0.49$, $p = 0.06$) in primary ProgMS. Since the lateral corticospinal tract is responsible for motor control of the limbs, a correlation between lateral funiculi MHI and EDSS and/or 9HPT is expected. High MHI in the dorsal column could be associated with reduced dexterity (cuneate fasciculus) and balance (gracile fasciculus), reflecting demyelination in large, heavily myelinated fibers of the ascending proprioceptive pathways. Previous studies using animal models have found that damage to cuneate fasciculus of the dorsal column disrupted fine movement control of fingers and impaired response to tactile stimuli of the hand.^{16,17} The absence of a significant correlation with disability in RRMS participants despite a wide range of MHI could be due to a shorter disease duration or greater capacity to repair in RRMS. It could also reflect that a certain threshold of damage to myelin is required before compensatory mechanisms start to fail.

Although myelin abnormality can be studied by comparing mean MWF (myelin content) between groups, there is substantial biological variation of myelin content between individuals.^{18,19} This confounds whether a lower mean MWF value, for example, in an MS patient, can be attributed to myelin loss from disease processes rather than natural inter-individual variation. The MWF variance (myelin heterogeneity) within an ROI may help mitigate this limitation. MHI incorporates both the mean and variance of MWF. Either low mean MWF or high MWF variance would result in a high MHI, indicative of myelin abnormality. Partial demyelination along a tract would decrease the mean MWF and increase the heterogeneity. Since MHI captures a change in mean and variance, it is more sensitive to myelin damage than using mean MWF alone, particularly in cross-sectional studies with limited sample size. Recently, Abel et al.²⁰

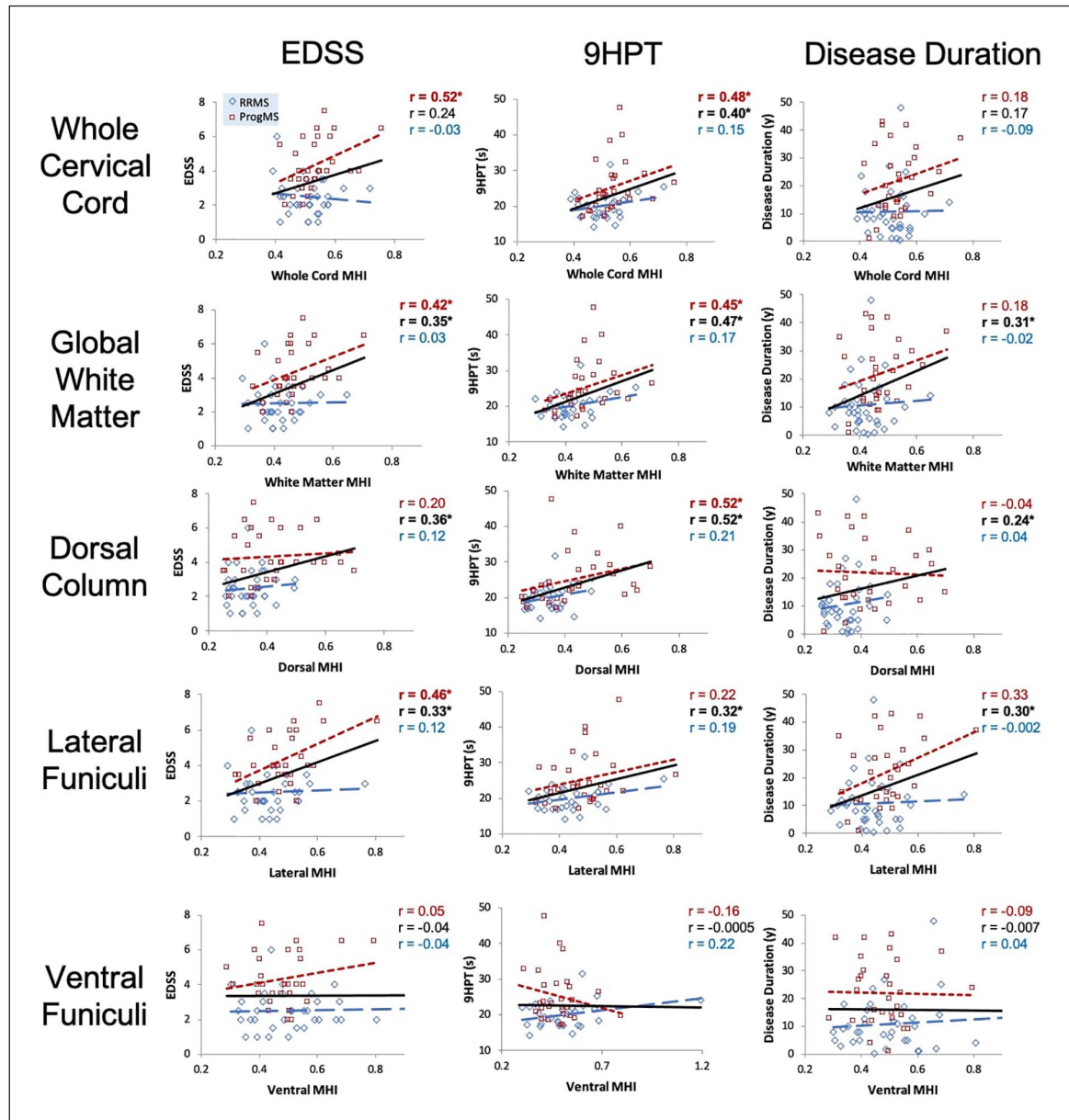


Figure 3. Correlations between MHI and EDSS (left column), 9-Hole Peg Test (9HPT) (middle column) and disease duration (right column) in (from top to bottom) whole cervical cord, global white matter, dorsal column, lateral funiculi, and ventral funiculi at C2/C3 level across relapsing-remitting MS (blue) and progressive MS (red). Spearman coefficients are reported for all MS (solid black), relapsing-remitting MS (dashed blue), and progressive MS (dotted red) and marked with an asterisk (*) if $p < 0.05$. Please note that x-axes are uniform, except 9HPT versus ventral funiculi MHI plot.

showed that MWF variance was higher in MS and more consistent between healthy individuals than mean MWF. They also found an inverse relationship between myelin heterogeneity and cognitive processing speed performance in MS, which was not significant using the mean MWF.²⁰ Furthermore, Wearn *et al.*²¹ proposed that T2 heterogeneity in the brain may be a superior measure than mean T2 to predict cognitive decline and to be used as an early marker of Alzheimer's disease pathology. These past findings

support that MHI may be a more sensitive metric to detect subtle alterations in cervical cord myelin that may not be evident with mean MWF measures alone.

Despite the importance of the spinal cord involvement in MS, fewer MRI studies have been performed in the spinal cord than the brain due to inherent technical challenges.²² Specifically, the spinal cord has small cross-sectional dimensions and is prone to artifacts due to motion, flow, and magnetic

Table 2. Inter-participant mean, SD, and COV for the MHI within each region of interest.

	HC (<i>n</i> =28)			RRMS (<i>n</i> =35)			ProgMS (<i>n</i> =30)		
	Mean	SD	COV	Mean	SD	COV	Mean	SD	COV
Whole cervical cord MHI	0.49	0.07	0.15	0.51	0.07	0.14	0.54	0.07	0.14
Global white matter MHI	0.40	0.07	0.18	0.42	0.07	0.17	0.47	0.08	0.17
Dorsal column MHI	0.33	0.07	0.22	0.34	0.06	0.18	0.43	0.13	0.29
Lateral funiculi MHI	0.41	0.09	0.22	0.44	0.09	0.21	0.48	0.10	0.20
Ventral funiculi MHI	0.48	0.09	0.20	0.51	0.17	0.33	0.48	0.10	0.21

SD: standard deviation; COV: coefficient of variation; MHI: myelin heterogeneity index; RRMS: relapsing-remitting multiple sclerosis; ProgMS: progressive multiple sclerosis; HC: healthy control.

susceptibility.²² However, recent technical advancements have made spinal cord MRI possible with clinically feasible quality and acquisition time.⁶

Although magnetization transfer (MT) imaging and diffusion tensor imaging (DTI) have also been used to study spinal cord myelin *in vivo*, they are less pathologically specific than MWI.^{15,23,24} MT contrast is generated by the exchange of magnetization between mobile (free) water protons and immobile (restricted) protons bound to macromolecular proteins and lipids such as in myelin.²⁵ However, MT can also be affected by edema, inflammation, and axonal density.²⁶ In a previous study, MT metrics in the spinal cord had a weak correlation with EDSS.²⁷ DTI evaluates the directionality and magnitude of diffusivity of water molecules to provide information about neuron orientation and WM tissue integrity.²⁸ DTI measures have been shown to reflect myelin, fiber coherence, axonal density, and membrane permeability.^{29,30} In MS, radial diffusivity and fractional anisotropy were found to relate to 9HPT, T25W, and EDSS in the dorsal column and lateral funiculi, which supported our findings except for the T25W.³¹

Lesions were not removed from our regions since a correlation between MHI and the clinical measures should reflect the integrity of the whole tract including both normal-appearing and lesional tissue. Furthermore, previous work with MWI had shown little effect of removing lesions from analysis due to the relatively small volume and heterogeneous nature of the amount of demyelination in various lesions.³² However, inclusion of lesion volume/count and cord volume may increase sensitivity to disability measures and will be assessed in future studies with longitudinal data.

In this study, our data were collected at a single site using a single scanner, which may limit the generalizability of our results. However, previous MWI studies

demonstrated good intersite (mean MWF coefficient of variation (COV)=4.68 %) and inter-vendor (mean MWF COV=2.77 %) reproducibility.^{18,33} This supports the feasibility for multicenter studies to use MWI to further improve our understanding of the pathological processes in MS that may contribute to clinical disability. In addition, we included a heterogeneous population from different parts of the MS spectrum to represent a wide range of the real-world MS population. While the HC group was matched by sex and age to the MS group as a whole, the RRMS and ProgMS groups differed in terms of age, EDSS, and disease duration by the nature of the phenotypes. While sex and age (within this age range) have been shown to play only minor or negligible roles in MWF in healthy brain,³⁴ disease duration appears to play a more important role in ProgMS than RRMS in our cohorts (Figure 3); understanding the impact of these different characteristics of the groups warrants further exploration in a larger cohort. Another factor worthy of consideration is that we scanned the cervical cord, particularly C2/C3 level, rather than the whole spinal cord. While this may be considered a limitation, previous studies have shown that focal spinal cord damage (lesional tissue) in MS was most often found in the cervical region.³⁵ Restricting the imaging FOV to the cervical spine allows for higher image resolution and shorter acquisition time, which in turn helps to minimize motion artifacts and patient discomfort. The increased amount of vertebral bone lower in the thoracic spinal cord exacerbates artifacts from magnetic field inhomogeneity, such as signal loss and image distortion. The cervical cord, particularly the ventral funiculi region, is substantially smaller than the brain, making it more prone to partial volume effects. Therefore, MWI results from ventral funiculi should be interpreted with caution. Furthermore, while axonal loss and cord atrophy are clinically relevant, their presence indicates that tissue destruction has already taken place. Therefore, it would be clinically useful to measure myelin, which has the capacity to

repair and remyelinate, to determine the critical time window of opportunity to intervene to delay disease progression and prevent permanent disability.

Our findings support the efficacy of using GRASE-derived MWI metrics, acquired with a clinically feasible acquisition time of about 8 min, to study myelin pathology in the cervical spinal cord of MS. MWI provides an in vivo marker of myelin that can indicate the presence of myelin abnormality in the spinal cord of MS. This measurement supplements conventional (clinical) MRI findings by providing additional information about biological changes within normal-appearing and lesional tissue. Therefore, MWI could serve as a valuable tool for monitoring therapeutic effects, disease progression, tissue repair, and neuroprotection in MS and other diseases involving myelin pathology.

Acknowledgements

The authors sincerely thank all study participants and the MR technologists at the University of British Columbia MRI Research Center.

Declaration of Conflicting Interests


The author(s) declared no potential conflicts of interest with respect to the research, authorship, and/or publication of this article.


Funding

The author(s) disclosed receipt of the following financial support for the research, authorship, and/or publication of this article: This work was financially supported by the Multiple Sclerosis Society of Canada (grant no. F16-04023).

ORCID iDs

Lisa Eunyoung Lee  <https://orcid.org/0000-0002-8334-3740>

Adam Dvorak  <https://orcid.org/0000-0001-6107-5610>

Shawna Abel  <https://orcid.org/0000-0001-8547-1415>

Robert Carruthers  <https://orcid.org/0000-0001-7085-1001>

References

- MacKay A, Whittall K, Adler J, et al. In vivo visualization of myelin water in brain by magnetic resonance. *Magn Reson Med* 1994; 31(6): 673–677.
- Laule C, Leung E, Lis DK, et al. Myelin water imaging in multiple sclerosis: Quantitative correlations with histopathology. *Mult Scler* 2006; 12(6): 747–753.
- Wright AD, Jarrett M, Vavasour I, et al. Myelin water fraction is transiently reduced after a single mild traumatic brain injury: A prospective cohort study in collegiate hockey players. *PLoS ONE* 2016; 11(2): e0150215.
- Flynn SW, Lang DJ, Mackay AL, et al. Abnormalities of myelination in schizophrenia detected in vivo with MRI, and post-mortem with analysis of oligodendrocyte proteins. *Mol Psychiatry* 2003; 8(9): 811–820.
- Dvorak AV, Ljungberg E, Vavasour IM, et al. Rapid myelin water imaging for the assessment of cervical spinal cord myelin damage. *Neuroimage Clin* 2019; 23: 101896.
- Ljungberg E, Vavasour I, Tam R, et al. Rapid myelin water imaging in human cervical spinal cord. *Magn Reson Med* 2017; 78(4): 1482–1487.
- Thompson AJ, Banwell BL, Barkhof F, et al. Diagnosis of multiple sclerosis: 2017 revisions of the McDonald criteria. *Lancet Neurol* 2018; 17: 162–173.
- Kurtzke JF. Rating neurologic impairment in multiple sclerosis: An Expanded Disability Status Scale (EDSS). *Neurology* 1983; 33(11): 1444–1452.
- Cutter GR, Baier ML, Rudick RA, et al. Development of a multiple sclerosis functional composite as a clinical trial outcome measure. *Brain* 1999; 122(Pt. 5): 871–882.
- Prasloski T, Rauscher A, MacKay AL, et al. Rapid whole cerebrum myelin water imaging using a 3D GRASE sequence. *NeuroImage* 2012; 63: 533–539.
- Prasloski T, Mädler B, Xiang QS, et al. Applications of stimulated echo correction to multicomponent T2 analysis. *Magn Reson Med* 2012; 67(6): 1803–1814.
- Yoo Y, Prasloski T, Vavasour I, et al. Fast computation of myelin maps from MRI T2 relaxation data using multicore CPU and graphics card parallelization. *J Magn Reson Imaging* 2015; 41: 700–707.
- De Leener B, Lévy S, Dupont SM, et al. SCT: Spinal Cord Toolbox, an open-source software for processing spinal cord MRI data. *NeuroImage* 2017; 145: 24–43.
- De Leener B, Fonov VS, Collins DL, et al. PAM50: Unbiased multimodal template of the brainstem and spinal cord aligned with the ICBM152 space. *NeuroImage* 2018; 165: 170–179.
- Kolind S, Seddigh A, Combes A, et al. Brain and cord myelin water imaging: A progressive multiple sclerosis biomarker. *Neuroimage Clin* 2015; 9: 574–580.

16. Liao CC, DiCarlo GE, Gharbawie OA, et al. Spinal cord neuron inputs to the cuneate nucleus that partially survive dorsal column lesions: A pathway that could contribute to recovery after spinal cord injury. *J Comp Neurol* 2015; 523: 2138–2160.
17. Darian-Smith C. Monkey models of recovery of voluntary hand movement after spinal cord and dorsal root injury. *ILAR J* 2007; 48(4): 396–410.
18. Meyers SM, Vavasour IM, Mädler B, et al. Multicenter measurements of myelin water fraction and geometric mean T2: Intra- and intersite reproducibility. *J Magn Reson Imaging* 2013; 38(6): 1445–1453.
19. Vavasour IM, Clark CM, Li DKB, et al. Reproducibility and reliability of MR measurements in white matter: Clinical implications. *NeuroImage* 2006; 32: 637–642.
20. Abel S, Vavasour IM, Lee LE, et al. Myelin damage in normal appearing white matter contributes to impaired cognitive processing speed in multiple sclerosis. *J Neuroimaging* 2020; 30(2): 205–211.
21. Wearn AR, Nurdal V, Saunders-Jennings E, et al. T2 heterogeneity: A novel marker of microstructural integrity associated with cognitive decline in people with mild cognitive impairment. *Alzheimers Res Ther* 2020; 12: 105.
22. Stroman PW, Wheeler-Kingshott C, Bacon M, et al. The current state-of-the-art of spinal cord imaging: Methods. *NeuroImage* 2014; 84: 1070–1081.
23. MacKay AL and Laule C. Magnetic resonance of myelin water: An in vivo marker for myelin. *Brain Plast* 2016; 2: 71–91.
24. Ciccarelli O, Cohen JA, Reingold SC, et al. Spinal cord involvement in multiple sclerosis and neuromyelitis optica spectrum disorders. *Lancet Neurol* 2019; 18(2): 185–197.
25. Henkelman RM, Stanisz GJ and Graham SJ. Magnetization transfer in MRI: A review. *NMR Biomed* 2001; 14(2): 57–64.
26. Vavasour IM, Laule C, Li DKB, et al. Is the magnetization transfer ratio a marker for myelin in multiple sclerosis? *J Magn Reson Imaging* 2011; 33: 713–718.
27. Lycklama à Nijeholt GJ, Castelijns JA, Lazeron RHC, et al. Magnetization transfer ratio of the spinal cord in multiple sclerosis: Relationship to atrophy and neurologic disability. *J Neuroimaging* 2000; 10(2): 67–72.
28. Fox RJ, Cronin T, Lin J, et al. Measuring myelin repair and axonal loss with diffusion tensor imaging. *AJNR Am J Neuroradiol* 2011; 32(1): 85–91.
29. Beaulieu C. The basis of anisotropic water diffusion in the nervous system: A technical review. *NMR Biomed* 2002; 15(7-8): 435–455.
30. Harsan LA, Poulet P, Guignard B, et al. Brain dysmyelination and recovery assessment by noninvasive in vivo diffusion tensor magnetic resonance imaging. *J Neurosci Res* 2006; 83: 392–402.
31. Naismith RT, Xu J, Klawiter EC, et al. Spinal cord tract diffusion tensor imaging reveals disability substrate in demyelinating disease. *Neurology* 2013; 80: 2201–2209.
32. Combes AJE, Matthews L, Lee JS, et al. Cervical cord myelin water imaging shows degenerative changes over one year in multiple sclerosis but not neuromyelitis optica spectrum disorder. *Neuroimage Clin* 2017; 16: 17–22.
33. Lee LE, Ljungberg E, Shin D, et al. Inter-vendor reproducibility of myelin water imaging using a 3D gradient and spin echo sequence. *Front Neurosci* 2018; 12: 854.
34. Dvorak A, Swift-LaPointe T, Vavasour I, et al. An atlas for human brain myelin content throughout the adult life span. *Sci Rep* 2021; 11: 269.
35. Eden D, Gros C, Badji A, et al. Spatial distribution of multiple sclerosis lesions in the cervical spinal cord. *Brain* 2019; 142: 633–646.